



Title	Relationship between latent heat of sea spray and uncertainty of a meteorological field
Author(s)	Saruwatari, Ayumi; Abe, Nobuhiro
Citation	Applied Ocean Research, 44, 102-111 https://doi.org/10.1016/j.apor.2013.11.007
Issue Date	2014-01
Doc URL	http://hdl.handle.net/2115/53976
Type	article (author version)
File Information	elsarticle-template-harv-1.pdf



[Instructions for use](#)

Relationship Between Latent Heat of Sea Spray and Uncertainty of a Meteorological Field

Ayumi Saruwatari^{a,*}, Nobuhiro Abe^b

^a*Faculty of Engineering, Hokkaido University, Sapporo, Japan.*

^b*Hokkaido Hitachi Systems, Sapporo, Japan*

Abstract

A surf zone with large breaking waves produces more spray than do offshore regions. Latent heat of spray evaporation causes change in the surrounding temperature and wind velocity, resulting in further alterations in temperature, wind velocity and heat flux. Spray in a surf zone with large breaking waves may have unignorable effect on determination of a local meteorological field because of this interconnected relationship as well as its higher population than in the open ocean. In this study, the effects of the spray latent heat on a meteorological field were investigated. The authors propose a method for estimating latent heat of spray vaporization over the ocean. The method was applied to a meso-scale meteorological model to perform numerical experiments with consideration of heat flux by spray. Although the contribution of heat flux on the ocean was as small as 2.5%, fluctuations of air temperature and wind velocity increased over time due to the effects of spray. The fluctuations are thought to cause uncertainty in weather prediction. Numerical experiments with spray provided predictions of air temperature and wind velocity near a coast line that were consistent with observational data, especially when the population of spray droplets increased by two orders of magnitude as is often observed in a coastal area.

Keywords: Air-sea heat transfer, coastal meteorology, sea spray, Weather Research and Forecasting model

1. Introduction

Heat exchange between the air and ocean is represented by the sum of direct exchange through the ocean surface and exchange by evaporation of sea spray. Sea spray accelerates the air-sea heat transfer by evaporating as soon it emerges since it has a large surface area compared to its volume, and its large surface curvature accelerates the evaporation process. Sea spray arises through several different mechanisms. Most of the spray on the open ocean arises in a bubble bursting process (e.g. Spiel, 1998; Günther et al., 2003). Air bubbles entrained in the water by whitecapping burst on the sea surface causing the generation of so-called ‘film droplets’ and subsequently ‘jet droplets’ having sizes of $O(1-10 \mu\text{m})$ depending on the sizes of the bubbles. A strong wind blowing over waves causes the generation of ‘spume’ droplets (e.g. Veron et al.,

*Corresponding Author

Email address: saruwata@eng.hokudai.ac.jp (Ayumi Saruwatari)

Preprint submitted to Applied Ocean Research

January 6, 2014

2012) with sizes of $O(100 \mu\text{m})$ by tearing off the water surface on the wave crest. Andreas (1998) noted that the threshold of a 10-m wind speed to form spumes is in the range of 7–11 ms^{-1} . Experimental results obtained by Anguelova et al. (1999) showed that the number of spume droplets sharply increases with a 10-m wind speed of more than 23 ms^{-1} . Spumes therefore are less dominant under a moderate wind condition. Depth-induced breaking waves cause production of spray in a coastal area since the jet of a breaking wave fragments into droplets through interaction between the water surface and vortices underneath the surface (Saruwatari et al., 2009). In addition, aeration induced by jet splashing intensifies production of film and jet droplets in a surf zone. The size and population of spray droplets produced in a wave-breaking process are still indefinite because spray in a surf zone is produced through various mechanisms. de Leeuw (1999) observed that the number density of sea spray droplets of more than $O(10 \mu\text{m})$ in size in a surf zone was one to two orders of magnitude larger than that in the offshore region under a moderate wind condition, which is thought to be because of continuous aeration and spray production concentrated in a surf zone (Figs 2 and 3 of Saruwatari et al., 2009). According to the relationship between evaporation velocity and falling velocity of spray, the most effective spray droplet size for heat transfer is $O(10\text{--}100 \mu\text{m})$ (Andreas, 1992), which coincides with the size range of spray droplets produced in a surf zone. Sea spray in a coastal region is presumably more important for determination of local meteorology than that in an offshore region.

Multitudes of spray generation functions (SGFs; also known as sea-spray source function, S3F), representing the number and size distribution of spray droplets emerging from the ocean, have been proposed (e.g. O’Dowd and de Leeuw, 2007). Although the number and size distributions of spray depend on the wind condition, wave condition as well as the water properties such as the surface tension and salinity, most SGFs are parametrized only by wind speed since it is the most dominant factor to determine the spray population in offshore region. Spray generation functions have been developed based on the data obtained by observations in the open ocean to quantify the spray population in offshore regions, not for the purpose of quantifying the spray population in a coastal area. In order to represent the increase in spray population in a coastal area, it may be better to include a parameter of the ocean such as wave height or fetch in an SGF model. de Leeuw et al. (2000) proposed an SGF model based on their observations performed near a surf zone. Piazzola et al. (2002, 2009) also quantified the amount of film and jet droplets in a coastal area by focusing on the change in whitecap coverage under a short fetch condition. The size and number of spray droplets in a coastal area, however, are not fully understood.

Air-sea heat flux for weather prediction is usually given by a bulk model (e.g. Vickers and Mahrt, 2006) that is constructed on the basis of data from offshore observations parametrized by wind speed. Although the models implicitly contain the contribution of sea spray, they cannot give accurate heat exchange in a coastal area that depends on local variations in the size and number of spray droplets.

The final goal of our study is to understand and quantify the effects of sea spray on a local meteorological field above a coastal area. In this study, we focused on characterizing the effects of sea spray on meteorology above the ocean and the time variation of the effects. We investigate how meteorological field changes by responding to the increase of spray population up to 100 times as much as that in a normal state of the open ocean. We developed a method to estimate the latent heat flux of sea spray, and the method was embedded into a meteorological model as shown in §2. We performed numerical experiments to investigate how meteorological fields are affected by the spray population (§3–§5). The results of numerical experiments showed that a small difference in air temperature caused by the spray latent heat is amplified with time to form an entirely different meteorological field. We also discuss the possibility of more accurately

predicting coastal meteorology by considering the latent heat of spray in a coastal area (§6).

2. Latent Heat of Sea Spray

2.1. Calculation method

Latent heat of evaporation through a water surface q_{sf} is generally obtained by multiplying the latent heat coefficient L and evaporation speed w :

$$q_{sf} = Lw, \quad (1)$$

where the evaporation speed should be determined on the basis of the ambient environment. We applied the following empirical model for determining the evaporation velocity in a turbulent flow (Ueda, 2000, 1960):

$$w = 0.0018 \frac{K}{\nu} u (e_s - e) \times 10^{-2} \quad [\text{kg m}^{-2}\text{s}^{-1}], \quad (2)$$

where K [m^2s^{-1}] represents the diffusion coefficient for water vapor, ν [m^2s^{-1}] is the kinematic viscosity coefficient, u [m s^{-1}] is the ambient air velocity over the surface, e_s [Pa] is the saturated vapor pressure of water on the surface and e [Pa] is the ambient vapor pressure. We used the terminal velocity w_t of a falling droplet calculated as explained later for the ambient velocity, assuming horizontal velocity of a droplet is identical to the wind speed. The saturated vapor pressure on the curved water surface was obtained from Kelvin's equation:

$$e_s = e_{s0} \exp\left(\frac{2\sigma}{re_s}\right), \quad (3)$$

where σ is the coefficient of surface tension and r is the radius of the curvature represented by the radius of the spray droplet. The saturated vapor pressure on a still water surface e_{s0} [Pa] was determined on the basis of the approximation of Murray (1967):

$$e_{s0} = 610.78 \exp\left(\frac{aT_a}{T_a + b}\right), \quad (4)$$

where T_a [$^{\circ}\text{C}$] is ambient temperature, and $a = 17.27$ and $b = 237.30$ are coefficients. The ambient vapor pressure e was obtained using specific humidity S :

$$e = \frac{M_{air}}{M_{vapor}} pS, \quad (5)$$

where M_{air} and M_{vapor} represent the molecular weights of air and vapor, respectively, and p is ambient pressure.

The latent heat flux from the surface area of a droplet obtained from eq. (1) is integrated over the whole surface area of the spray droplets distributed over the ocean to estimate the net latent heat flux from the ocean surface H_{sp} .

$$H_{sp} = \int_{r_{min}}^{r_{max}} 4\pi r_0^2 q_{sf} \tau \frac{dF}{dr_0} dr_0, \quad (6)$$

where r_{min} and r_{max} represent the minimum and maximum spray droplet radii at the formation. We considered droplets with the initial radii between 0.1 and 300 μm that is typical size range of sea spray (e.g. Günther et al., 2003; Andreas, 2005). τ is the duration of heat transfer, and dF/dr is a sea-spray source function representing the number density flux of sea spray droplets with radii of r . The shorter time between the time during which spray stays in the air τ_f and the time required for all moisture in a droplet to evaporate τ_e is chosen for the duration of heat transfer τ .

$$\tau = \min[\tau_f, \tau_e], \quad (7)$$

$$\tau_f = \frac{h_0}{w_t}, \quad (8)$$

$$\tau_e = \frac{r\rho}{3w}, \quad (9)$$

where h_0 is the initial height of a droplet from the sea surface, which was reported to be 5–20 cm by Blanchard and Woodcock (1957) and 15–20 cm by Spiel (1998) for film and jet droplets based on the experiments. We defined h_0 as 15 cm in the present study by roughly taking an average of their experimental results. w_t is the terminal velocity of a falling droplet, which is determined by a relationship between gravity, buoyancy and drag forces:

$$w_t = \left(\frac{8gr(\rho_{sea} - \rho_{air})}{3C_D\rho_{air}} \right)^{1/2} \quad (10)$$

$$C_D = \begin{cases} 24/Re & (r \leq 140\mu\text{m}) \\ 0.44 & (\text{otherwise}) \end{cases} \quad (11)$$

where ρ_{sea} and ρ_{air} are the densities of sea water and air, respectively, g is gravitational acceleration, $Re = \rho_{air}rV/\eta$ is the Reynolds number, $V = w_t$ is the velocity of the droplet, η is the air viscosity, and C_D is the drag coefficient that varies with droplet radius and also with the Reynolds number.

A saline droplet is known to reach an equilibrium radius in the evaporation process due to increase of salinity in the droplet (Fairall et al., 2009) although we assumed all moisture in a droplet can evaporate completely. This may cause overestimation of latent heat of sea spray. Here we discuss the possible effect of salinity on spray latent heat. We estimated latent heat of saline spray using equilibrium spray size calculated based on Andreas (2005). Latent heat of salty spray was 21% smaller than that estimated with eq. (6) under a typical meteorological condition in the present numerical experiment which is explained in the following section. Although a certain difference can appear by salinity, we ignored the effect of salinity and focused on investigating response of coastal meteorology to change in spray population in this study.

Spray source function proposed by Gong (2003) that is simply parametrized by wind speed was used in this study since the function can be applied to conditions of high wind velocity comparing to other SGF models (O'Dowd and de Leeuw, 2007).

$$\frac{dF}{dr} = 1.373U_{10}^{3.41}r^{-A} \left(1 + 0.057r^{3.45} \right) \times 10^{1.607 \exp(-B)}, \quad (12)$$

$$A = 4.7(1 + \theta r)^{-0.017r^{-1.44}}, \quad (13)$$

$$B = (0.433 - \log r) / 0.433. \quad (14)$$

Here $\theta = 30$ is a constant and U_{10} is the wind velocity at 10 m above the ocean. This model is thought to be applicable to a 10-m wind speed up to at least 17 ms^{-1} since the number size distribution of sea spray predicted by the model showed good agreement with observations under conditions of $U_{10} \leq 17 \text{ ms}^{-1}$ in his paper although no application range was specified. Gong (2003) modified a source function proposed by Monahan et al. (1986) in order to account for production of submicron droplets. O’Dowd and de Leeuw (2007) compared several source functions including this function and confirmed that estimated spray productions more than $0.1 \mu\text{m}$ were almost in a same order of magnitude, indicating Gong’s function is reasonable comparing to the other functions.

The latent heat flux of sea spray calculated by eq. (6) is given as a sea-surface boundary condition of a meteorological model to evaluate the effects of heat transfer due to the evaporation of sea spray as described later.

Meteorological conditions in which the present method can be applied for estimating latent heat of spray are dominated by the SGF used for calculation. Since the SGF used in this study was intended for spray generated through a bubble bursting process, it cannot be directly applied to a condition with high wind speed in which different mechanisms for spray generation also become dominant. Also, since strong wind more than 20 ms^{-1} enhances the vertical mixing of a marine boundary layer to transport spray droplets to several hundred meter upward (Shpund et al., 2011, 2012), heat flux by spray should not be applied as a surface boundary condition under strong wind conditions. The fetch should be sufficiently long as the SGF is supposed to predict the spray population in a sufficiently developed wind wave field. It may be also inappropriate to apply this method directly for a surf zone with dynamic breaking waves without modifying the SGF for the same reason that the dominant mechanism of spray generation is different from that in the open ocean.

2.2. Sensitivity of the latent heat of sea spray

Figure 1 shows the latent heat of spray vaporization calculated by the proposed method under various conditions of air temperature T_a , relative humidity RH and wind velocity at 10 m above the surface U_{10} in a range: $-10 \leq T_a \leq 20^\circ\text{C}$, $60 \leq RH \leq 90\%$ and $0 \leq U_{10} \leq 17 \text{ ms}^{-1}$. Humidity and temperature are main parameters for determining evaporation velocity, while wind speed is the main parameter for the spray source function. Wind speed was found to have greater effects than humidity and air temperature on latent heat of spray. Humidity (represented by S in eq. (5)) generally has more effects on determining evaporation speed w , as well as latent heat q_{sf} , over a flat water surface where a radius of curvature r in eq. (3) approaches infinity. The evaporation speed on a droplet surface with large surface curvature, however, turned out to be much greater and less dependent on humidity conditions than that on a flat water surface because of the small r in the eq. (3) (see eq.s (2)–(5)).

2.3. Comparison with other models

Figure 2 shows a comparison of latent heat flux of sea spray calculated by the present method with that estimated by methods proposed by Andreas (1992) and Perrie et al. (2005). Response of the latent heat of spray evaporation to wind velocity was qualitatively similar in all models, and quantitative difference between the models was almost within one order of magnitude. Andreas (1992) assumed spray evaporation in a thermal equilibrium for calculating latent heat of spray using parameters such as temperature, humidity and salinity. His estimations were more sensitive to a humidity condition than estimations using the present method. Perrie et al. (2005) applied

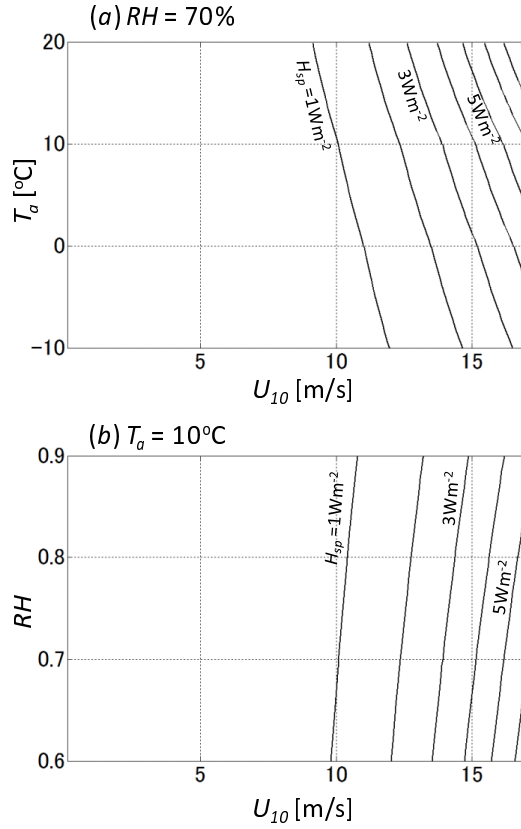


Figure 1: Contour of the spray latent heat calculated by the present method with various meteorological conditions with (a) constant humidity and (b) constant air temperature.

a simplified model for estimating latent heat of spray in their computation for investigating the contribution of sea spray to the development of a cyclone. Their model ignores the effects of surrounding conditions such as temperature and humidity for estimating spray latent heat in order to reduce computational costs. Although all of these models output spray latent heat in a same order of magnitude under most conditions, this study adopted the present method that estimates spray latent heat by considering the physical process of spray evaporation with relatively low computational costs.

3. Numerical Experiments

3.1. Meso-scale meteorological model

Wind and temperature fields are computed using a meso-scale meteorological model, Weather Research and Forecasting model (WRF-ARW, ver. 3.3.2). The initial and boundary conditions are based on reanalysis data, FNL global analysis data, having $1.0^\circ \times 1.0^\circ$ resolution and provided every six hours from National Centers for Environmental Prediction (NCEP). Real-Time Global

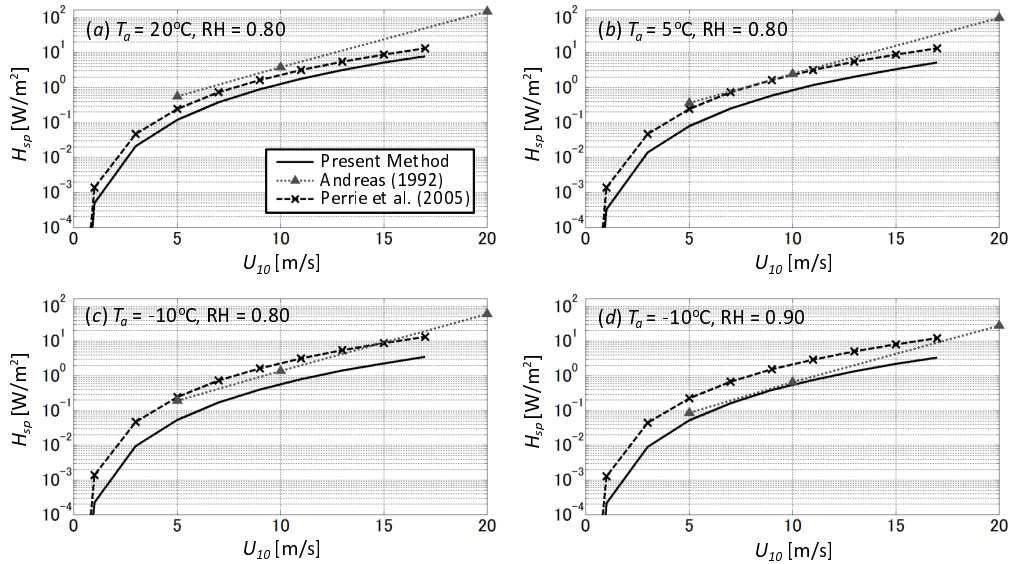


Figure 2: Comparison of the latent heat of sea spray estimated by the present method, the method of Andreas (1992) and the method of Perrie et al. (2005) under the conditions of the air pressure $p = 1000$ hPa and (a) $T_a = 20^\circ\text{C}$, $RH = 80\%$, (b) $T_a = 5^\circ\text{C}$, $RH = 80\%$, (c) $T_a = -10^\circ\text{C}$, $RH = 80\%$ and (d) $T_a = -10^\circ\text{C}$, $RH = 90\%$.

SST analysis data (RTG-SST) having $1/12^\circ \times 1/12^\circ$ resolution and provided every 12 hours by NCEP are also used for the boundary condition of sea surface temperature. The latent heat flux of spray evaporation estimated as explained above is applied as a boundary condition of heat flux through the ocean surface, in addition to the boundary conditions of heat flux given by a bulk model.

Typical options for computations of this scale were used in the WRF model, that is, a single-moment six-class scheme for microphysics (Hong and Lim, 2006), rapid radiative transfer model for long wave radiation (Mlawer et al., 1997), Goddard's scheme for short wave radiation (Chou and Suarez, 1994), Mesoscale Model (MM5) similarity theory for a surface layer (Zhang and Anthes, 1982), NOAA land surface model (Chen and Dudhia, 2001), Yonsei University scheme for a planetary boundary layer (Hong et al., 2006) and the Kain-Fritsch scheme for cumulus parametrization (Kain, 2004).

3.2. Computational conditions

The numerical experiments were conducted around Hokkaido, Japan, facing both the Pacific Ocean and Japan Sea (Fig. 3) since we can obtain observational data measured by Japan Meteorological Agency (JMA). The computational period was 12 hours from 0600 UTC 25 October 2009. This area has stable winds from the south-east direction as well as relatively large ocean waves with heights of 2–4 m having continuous production of spray due to whitecapping in a developed wave field during this season. A moderate wind ($U_{10} < 16 \text{ ms}^{-1}$) was blowing from the south-east direction for about 24 hours from 1800 on 24 October 2009. A fully developed

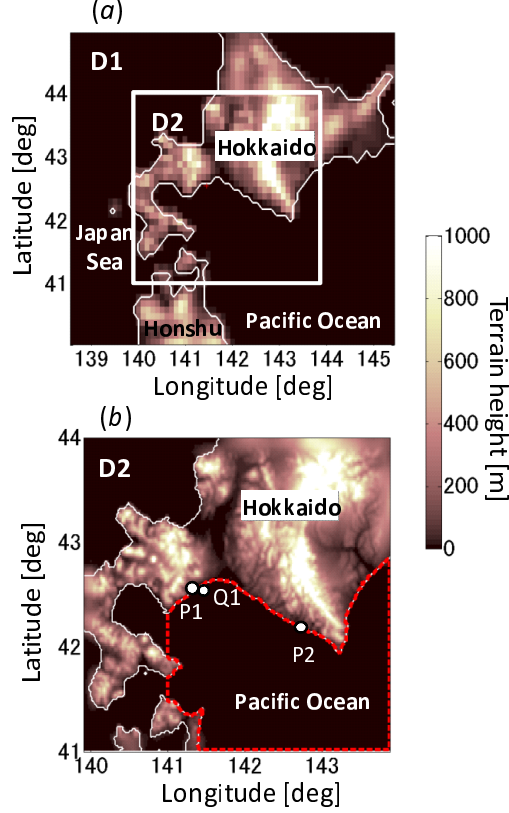


Figure 3: Computational domains: (a) domain 1 and (b) domain 2. Broken line in (b) represents the target area of the analysis.

wave field is known to have a constant Charnock coefficient a around 0.023 (Hsu, 1986):

$$a = \frac{2\pi H_s}{g T_s^2}, \quad (15)$$

where H_s is the significant wave height and T_s is the significant wave period. The Charnock coefficient at $Q1$ was calculated using wave data NOWPHAS (Nationwide Ocean Wave information network for Ports and HARbourS) provided every 20 min by Port and Airport Research Institute of Japan. The Charnock coefficient during the computational period was 0.027 on average with the standard deviation of 0.004. Wind waves were therefore fully developed, and wind and waves were at equilibrium for the fetch on the Pacific side. The meteorological conditions were suitable for applying the proposed method.

We performed nesting computations with two domains having 6.0 and 1.2 min grid resolutions, respectively, (Table 1) to conduct five cases of numerical experiments shown in Table 2. Computational time steps for the domains 1 and 2 were 60 and 12 sec, respectively. Case 1 corresponds to ordinary computation by the WRF model without considering any extra effects

Table 1: Computational domains.

Domain	Grid number (lon × lat × vert)	Grid interval [min × min]	Time step [s]
1	71 × 51 × 34	6.0 × 6.0	60
2	201 × 151 × 34	1.2 × 1.2	12

Table 2: Computational cases.

Case	Description
1	Default computation of WRF model
2	SGF proposed by Gong (2003)
3	10-times larger SGF than case 2
4	30-times larger SGF than case 2
5	100-times larger SGF than case 2

of sea spray. Additional heat flux by spray evaporation was applied on the sea surface in case 2 using the proposed method. Cases 3–5 are numerical experiments to determine the response of the meteorological field to an increase in the spray population by one to two orders of magnitude, with the original SGF being increased by factors of 10, 30 and 100 assuming no change in the spectrum form of spray size, which we defined as a model of increasing spray production in a surf zone (Fig. 4). van Eijk et al. (2011) parametrized spray production near a surf zone in terms of mean waveheight on the basis of their field observation of spray concentration in a coastal area. Spray source function calculated by their parametrization using the NOWPHAS data at $Q1$ is also plotted on Fig. 4. Cases 4–5 are thought to be roughly representing spray production around a coastal area from the comparison of the SGFs with the parametrization by van Eijk et al. (2011). We investigated sensitivity of the meteorological field to change in the population of spray droplets and determining the relative effects of spray instead of quantifying the contribution of spray with this model. Twelve-hour spin-up computation was performed beforehand without considering the heat flux by spray in all cases. We defined t as the time from 0600 on 25 October 2009. The computational results before $t = 12$ hr were analyzed in this study since temperature distribution in cases 2–5 starts deviating from the boundary conditions given by the reanalysis data due to the additional heat flux by spray evaporation at $t > 12$ hr.

4. Effects of Spray on the Meteorological Fields

Figure 5 shows evolutions of 10-m wind velocity U_{10} , air temperature at 2 m above the surface T_a and sea surface temperature T_s in case 1, presenting an overview of the meteorological field during the computational period. Wind velocity over the ocean was almost stable throughout the period with a mean velocity of 8.4 ms^{-1} and maximum velocity of 16.0 ms^{-1} . Landward wind was dominant at the Pacific Ocean side of domain 2 to form a developed wind wave field. We defined this area as a target area for analyzing the computational results (see Fig. 3). Heat transfer from the sea to air was dominant since the air temperature in the target area ($10.9\text{--}16.9^\circ\text{C}$) was

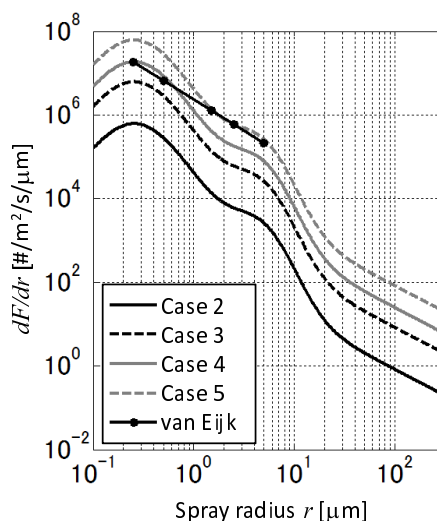


Figure 4: Spray source function given in case 2–5 when $U_{10} = 8.4 \text{ ms}^{-1}$ (based on Gong, 2003) and a source function by van Eijk et al. (2011).

lower than the sea surface temperature ($13.1\text{--}21.8^\circ\text{C}$) and the air on the ocean was relatively dry with mean relative humidity of 71.0% during the period.

Figure 6 shows the difference in air temperature near the surface ΔT_a in cases 2 and 5 from that in case 1. The air temperature over the ocean decreased with increase in wind speed in all cases. Air temperature on the land also decreased in a coastal area with significant landward wind. Although the mean temperature difference in case 2 was $O(-0.01^\circ\text{C})$ at first ($t = 3 \text{ hr}$), local disturbance of temperature amplified over the computational period, resulting in an intricate distribution of temperature difference ($t = 12 \text{ hr}$). This spatial fluctuation of temperature induced by spray latent heat is thought to cause uncertainty for weather prediction by a meteorological model. On the other hand, a more obvious temperature difference of $O(-1^\circ\text{C})$ arose in case 5 as soon spray latent heat was added to the surface boundary condition. Increase in the spray population in a surf zone by two orders of magnitude, therefore, presumably affects the local meteorological field around the coastal area. The relationship between mean/maximum temperature difference over the ocean and multiplying factor of the spray population in each case is shown in Fig. 7. Mean temperature difference increased with the spray population with a slope of 0.997. Vertical profiles of the temperature difference are shown in Fig. 8 for cases 2 and 5. Each line of the figure represents the temperature difference that is averaged over the region having 10-m wind velocity 3.0 ± 0.5 , 6.0 ± 0.5 , 9.0 ± 0.5 and $12.0 \pm 0.5 \text{ ms}^{-1}$. The additional heat flux due to spray also caused temperature fluctuation at a higher altitude. Perrie et al. (2005) reported that the heat flux of sea spray causes air temperature to decrease at a lower altitude and to increase at a higher altitude in cyclones. The present results showed that a decrease in air temperature on the surface causes oscillation of the temperature in the vertical direction.

The temperature difference caused alteration of wind velocity. Figure 9 shows the wind velocity differences in cases 2 and 5. Undulation of wind velocity difference that originated at a coast line developed with time in case 2. Although similar undulation can be seen near the coast in

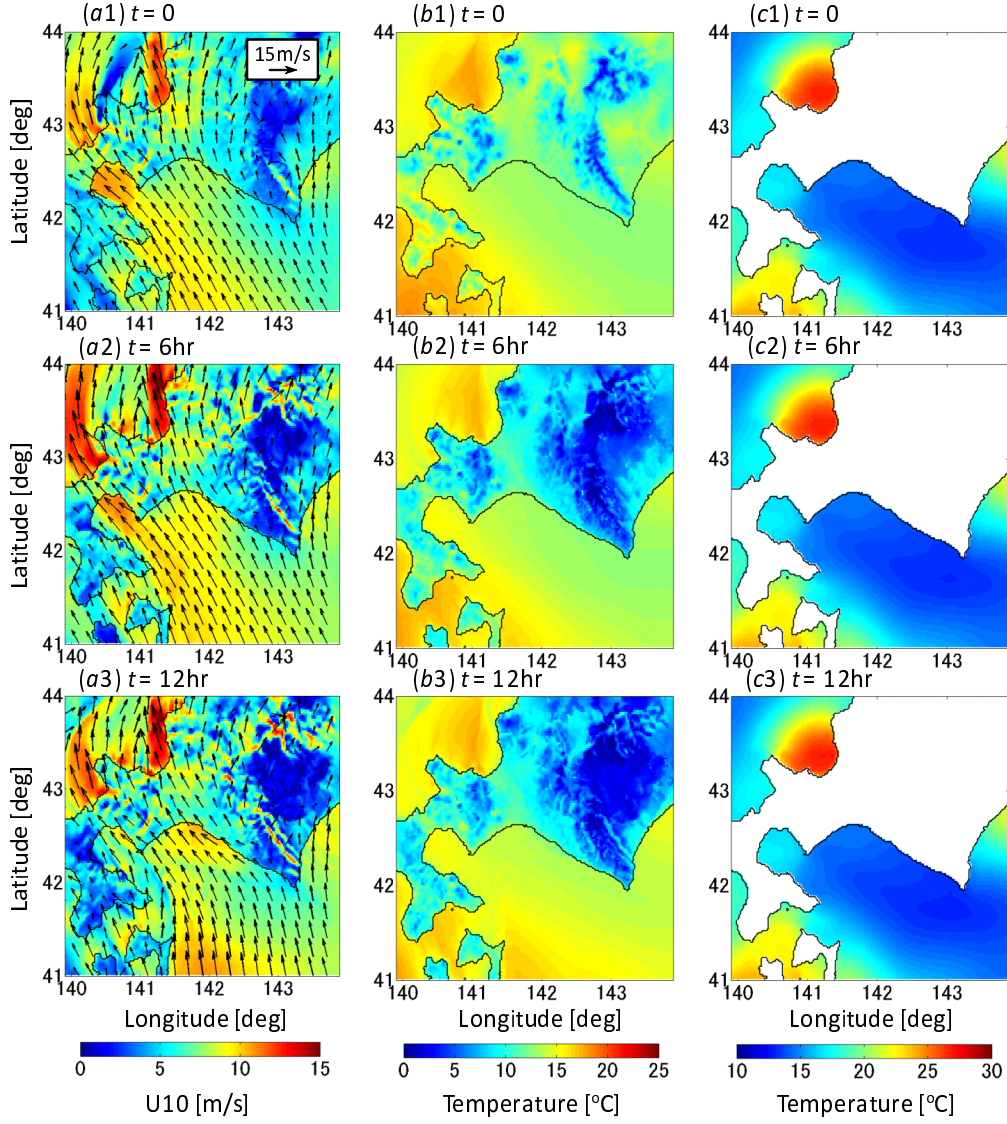


Figure 5: Distributions of (a) wind velocity U_{10} , (b) air temperature near the surface T_a and (c) sea surface temperature T_s at $t = 0, 6$ and 12 hr in case 1.

case 5, velocity depression in the offshore area of the Pacific Ocean side was more obvious with a larger spray population. The velocity difference increased over time, resulting in a maximum velocity difference of $O(1 \text{ ms}^{-1})$ by $t = 12$ hr. Andreas (2003) reported that an increase in number density of spray droplets under a high wind condition causes mechanical differences such as reduction of drag and friction on the surface that results in increase in wind speed. We found a certain velocity difference even when we simply considered only heat transfer due to spray

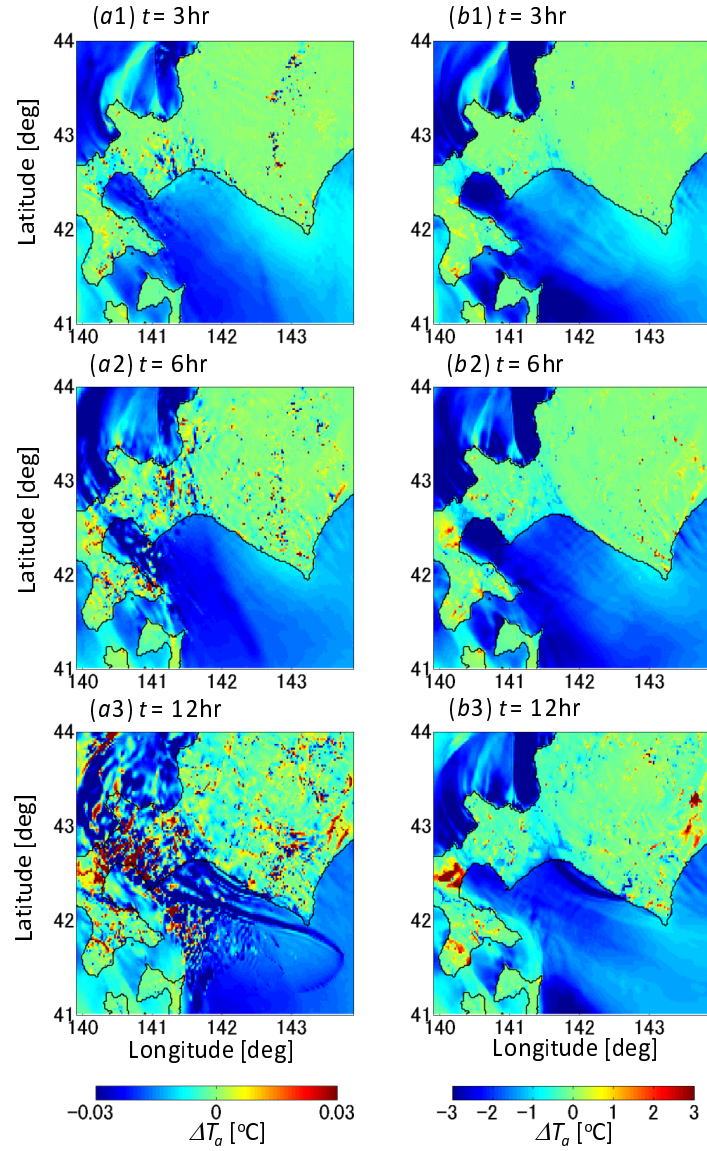


Figure 6: Distributions of air temperature at 2 m above the surface in (a) case 2 and (b) case 5 at $t = 3, 6,$ and 12 hr.

despite neglecting the mechanical contribution of spray. This velocity difference is thought to cause further differences in temperature and heat flux over the surface. The heat flux difference by latent heat of spray consequently affects the entire meteorological field since wind velocity, temperature and heat flux are interconnected.

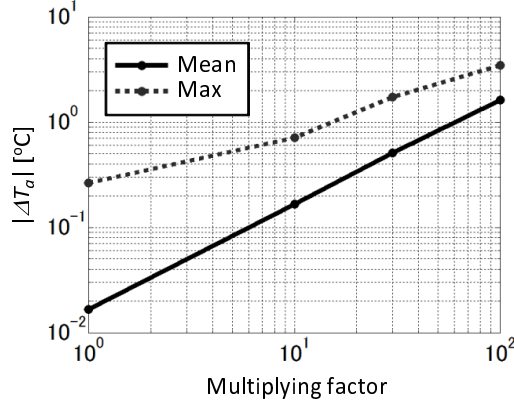


Figure 7: Relationship between the multiplying factor of SGF and mean/maximum temperature difference during $0 \leq t \leq 12$ hr that appeared over the target area in cases 2–5.

5. Contribution of Spray to Heat Flux

The total heat flux on the ocean surface calculated by the WRF model based on the surface layer model in case 1, which depends on the wind speed and air-sea temperature difference, was averaged over the target area (Fig. 10). Here, positive flux is defined as heat flux from the ocean to the air. Figure 11 shows the latent heat of spray additionally given on the sea surface in case 2. The maximum and minimum values that can be given under the present meteorological conditions are shown by error bars. Latent heat given in cases 3–5 is simply 10, 30 and 100 times that in Fig. 11, respectively. The latent heat in case 5, therefore, became $O(100 \text{ Wm}^{-2})$ with wind speed of more than 10 ms^{-1} , which is comparable to the original heat flux shown in Fig. 10 and also to the heat flux by spray in a cyclone given by Perrie et al. (2005).

Contribution of the latent heat of spray to the entire heat flux was also investigated in this study. Figure 12 shows the heat flux difference ΔH appeared by considering the spray latent heat. The data were normalized by the original heat flux in case 1 (H_0) and averaged over the target area for the computational period. Change in heat flux due to the latent heat of spray was 0–2.5% with wind speed of less than 15 ms^{-1} in case 2, while it increased to a maximum of 1.5 times the original heat flux in case 5 depending on the conditions of wind speed and temperature. The contribution of spray became more obvious with a smaller air-sea temperature difference since the entire heat flux becomes smaller with a small temperature difference (see Fig. 10). The effects of sea spray locally can be significant in a coastal area with large breaking waves that produce much spray even in a moderate meteorological condition without a storm since the contribution of spray increased with the spray population with a slope of 0.886–1.075 as shown in Fig. 13.

6. Comparisons with Observational Data

Figure 14 shows comparisons of wind speed and air temperature estimated by the present method and observational data provided every 10 min by the JMA at P1 and P2 indicated in

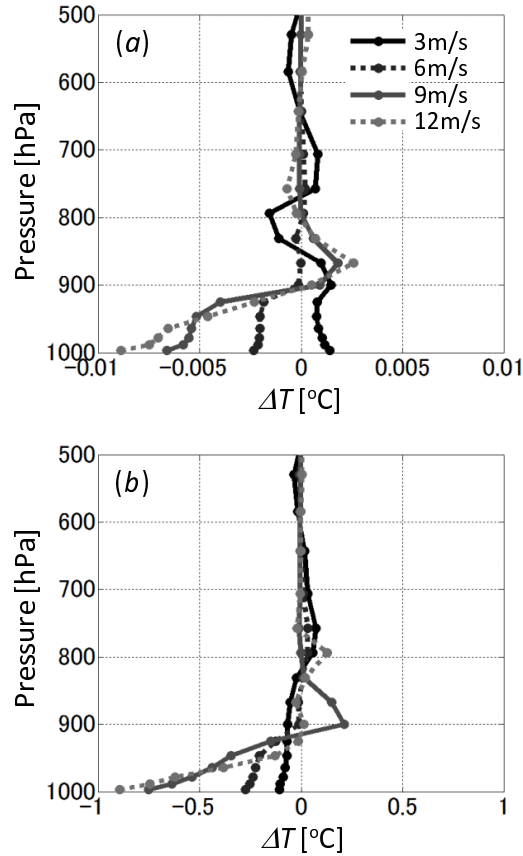


Figure 8: Vertical profiles of mean temperature difference over the target area in (a) case 2 and (b) case 5. Each plot represents a 10-m wind speed.

Fig. 3. P1 is near a beach used for surfing that has relatively large breaking waves producing much spray at any time, and both P1 and P2 are located only 20 m and 190 m, respectively, from the coast line. Since wind was blowing towards the land around the points, the meteorological field during this period, especially at P1, was susceptible to spray. The air temperatures at P1 and P2 were reproduced better in cases 2–5 than in case 1. Temporal fluctuations in both wind velocity and air temperature were more obvious in the computational results in case 5. Exclusion of spray latent heat causes uncertainty of weather prediction by a meteorological model with the current bulk model as shown previously. It is thought that spatial and temporal fluctuations of meteorological fields can be predicted more accurately by considering the effects of sea spray.

7. Conclusion

A method for estimating latent heat of spray evaporation over the ocean was proposed. The method was applied to a meso-scale meteorological model to perform numerical experiments for

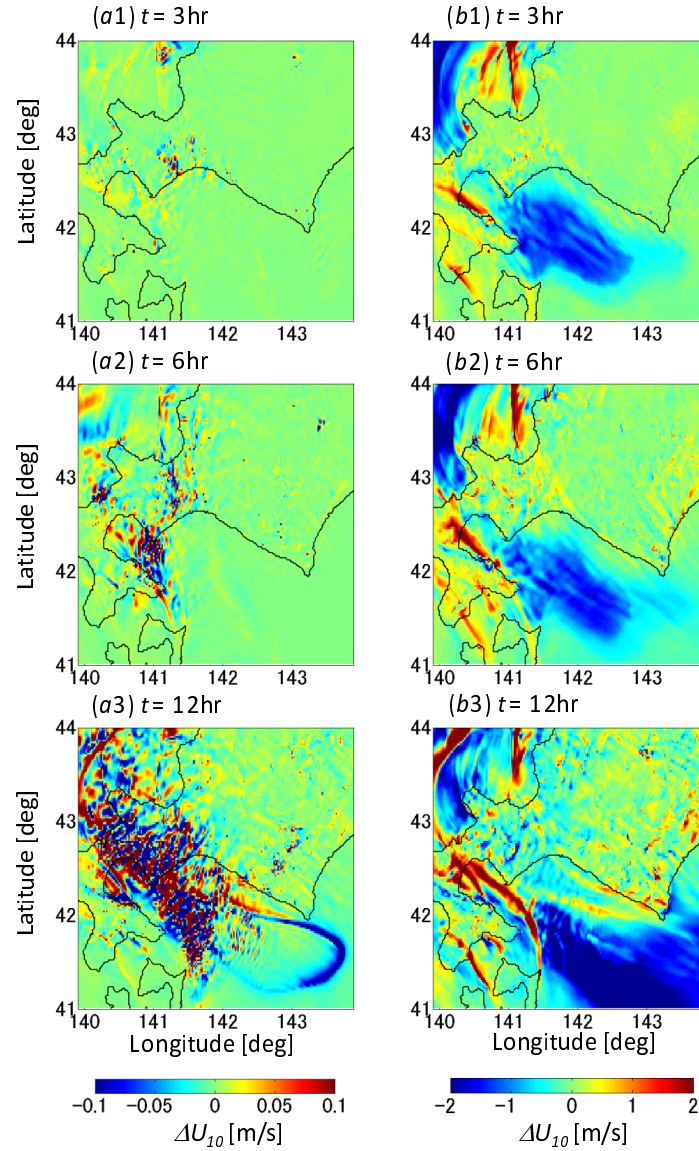


Figure 9: Distributions of difference in 10-m wind speed in (a) case 2 and (b) case 5 at $t = 3, 6,$ and 12 hr.

determining the effects of the latent heat of spray on meteorological fields.

Latent heat flux of spray caused depression of air temperature near the ocean surface, resulting in oscillation of air temperature at a higher altitude as well as wind velocity difference. Local disturbances of air temperature and wind velocity amplified over the computational period. Contribution of spray latent heat to the entire heat flux as well as depression of air temperature due to spray increased with the spray population. Air temperature in a coastal land area also decreased

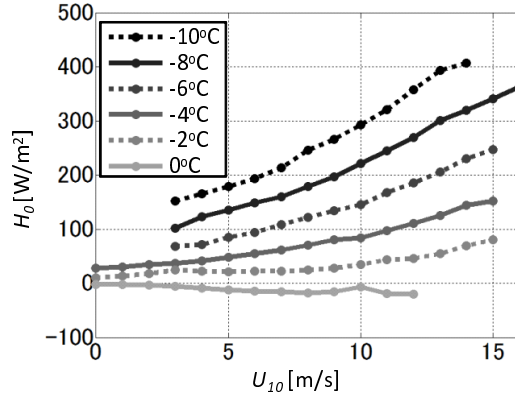


Figure 10: Total heat flux through the ocean surface in case 1. Each plot represents a different air-sea temperature difference ($T_a - T_s$).

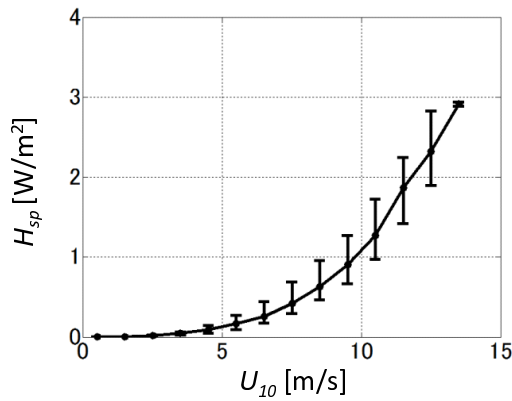


Figure 11: Latent heat flux of spray evaporation additionally given on the ocean surface as a boundary condition in case 2.

under a landward wind condition in the case of a large spray population. We compared the results of numerical experiments with wind and air temperature data obtained at locations near a coast line. Air temperature computed with the effects of spray latent heat showed better consistency with the observational data. Also, temporal fluctuations of air temperature and wind velocity were more obvious in cases with spray latent heat. Latent heat of sea spray, therefore, causes uncertainty in weather prediction by a meteorological model and affects local meteorological fields especially around a coastal area with a large spray population.

List of Symbols

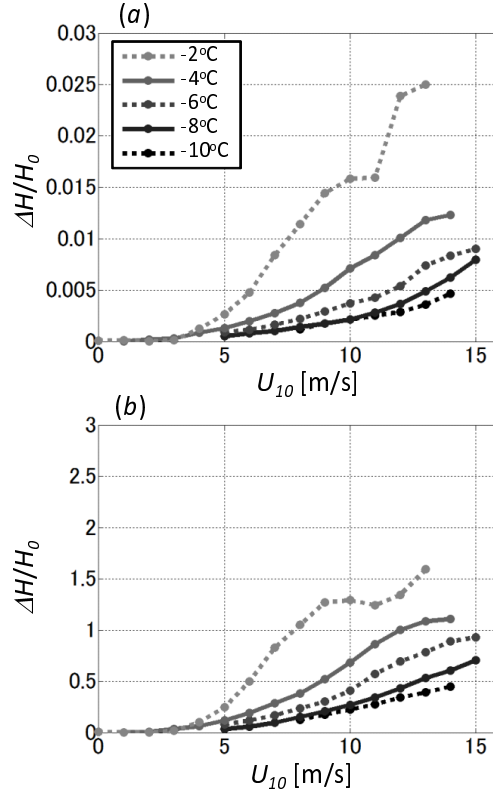


Figure 12: Relationship between fraction of heat flux difference and wind speed in (a) case 2 and (b) case 5. Each plot represents a different air-sea temperature difference ($T_a - T_s$).

C_D	Drag coefficient
dF/dr	Sea-spray source function [$\text{m}^{-2}\text{s}^{-1}\mu\text{m}$]
e_s	Saturated vapor pressure on a water surface [Pa]
e	Ambient vapor pressure [Pa]
e_{s0}	Saturated vapor pressure on a flat water surface [Pa]
H_0	Total heat flux through the ocean surface [W m^{-2}]
H_{sp}	Net latent heat flux from man ocean surface [W m^{-2}]
h_0	Initial height of a droplet [m]
K	Diffusion coefficient for water vapor [m^2s^{-1}]
L	Latent heat coefficient [J kg^{-1}]
M_{air}	Molecular weight of air
M_{vapor}	Molecular weight of vapor
p	Air pressure [Pa]
q_{sf}	Latent heat of evaporation through a water surface [W m^{-2}]
RH	Relative humidity
r	Radius of a spray droplet [m]

r_{min}	Minimum droplet radius [m]
r_{max}	Maximum droplet radius [m]
S	Specific humidity
T_a	Ambient temperature [°C]
T_s	Sea surface temperature [°C]
U_{10}	Wind velocity at 10 m above the ocean [m s^{-2}]
u	Ambient air velocity [m s^{-1}]
w	Evaporation speed [$\text{kg m}^{-2}\text{s}^{-1}$]
w_t	Terminal velocity of a falling droplet [m s^{-1}]
η	Air viscosity [Pa s]
ν	Kinematic viscosity coefficient [m^2s^{-1}]
ρ_{sea}	Sea-water density [kg m^{-3}]
ρ_{air}	Air density [kg m^{-3}]
σ	Coefficient of surface tension [N m^{-1}]
τ	Duration of heat transfer [s]
τ_e	Time for all moisture in a droplet to evaporate [s]
τ_f	Time for a droplet to stay in the air [s]

References

- Andreas, E. L., 1992. Sea spray and the turbulent air-sea heat fluxes. *J. Geophys. Res.* 97 (C7), 11429–11441.
- Andreas, E. L., 1998. A new sea spray generation function for wind speeds up to 32 m s^{-1} . *J. Phys. Oceanogr.* 28 (11), 2175–2184.
- Andreas, E. L., 2003. An algorithm to predict the turbulent air-sea fluxes in high-wind, spray conditions. 12th Conf. on Interaction of the Sea and Atmosphere 3.4.
- Andreas, E. L., 2005. Approximation formulas for the microphysical properties of saline droplets. *Atmospheric Research* 75, 323–345.
- Angelova, M., Barber, R. P., Wu, J., 1999. Spume drops produced by the wind tearing of wave crests. *J. Phys. Oceanogr.* 29, 1156–1164.
- Blanchard, D. C., Woodcock, A. H., 1957. Bubble formation and modification in the sea and its meteorological significance. *Tellus* 9 (2), 145–158.
- Chen, F., Dudhia, J., 2001. Coupling an advanced land-surface/hydrology model with the Penn State/NCAR MM5 modeling system. Part I: Model description and implementation. *Mon. Wea. Rev.* 129, 569–585.
- Chou, M. D., Suarez, M. J., 1994. An efficient thermal infrared radiation parameterization for use in general circulation models. *NASA Tech. Memo* 104606 (3), 85–85.
- de Leeuw, G., 1999. Sea spray aerosol production from waves breaking in the surf zone. *J. Aerosol Sci.* 30 (Suppl. 1), S63–S64.
- de Leeuw, G., Neele, F. P., Hill, M., Smith, M. H., Vignati, E., 2000. Production of sea spray aerosol in the surf zone. *J. Geophys. Res.* 105 (D24), 24397–29409.
- Fairall, C. W., Banner, M. L., Peirson, W. L., Asher, W., Morison, R. P., 2009. Investigation of the physical scaling of sea spray spume droplet production. *Journal of Geophysical Research: Oceans* 114 (C10).
- Gong, S. L., 2003. A parameterization of sea-salt aerosol source function for sub- and super-micron particles. *Global Biogeochem. Cycles* 17 (4), 1097.
- Günther, A., Walchli, S., von Rohr, P. R., 2003. Droplet production from disintegrating bubbles at water surfaces. Single vs. multiple bubbles. *Int. J. Multiphase Flow* 29, 795–811.
- Hong, S. Y., Lim, J.-O. J., 2006. The WRF single-moment 6-class microphysics scheme (WSM6). *J. Korean Meteor. Soc.* 42, 129–151.
- Hong, S. Y., Noh, Y., Dudhia, J., 2006. A new vertical diffusion package with an explicit treatment of entrainment processes. *Mon. Wea. Rev.* 134, 2318–2341.
- Hsu, S. A., 1986. A mechanism for the increase of wind stress (drag) coefficient with wind speed over water surfaces: a parametric model. *J. Phys. Oceanogr.* 16, 144–150.
- Kain, J. S., 2004. The Kain-Fritsch convective parameterization: An update. *J. Appl. Meteor.* 43, 170–181.
- Mlawer, E. J., Taubman, S. J., Brown, P. D., Iacono, M. J., Clough, S. A., 1997. Radiative transfer for inhomogeneous atmosphere: RRTM, a validated correlated-k model for the longwave. *J. Geophys. Res.* 102 (D14), 16663–16682.

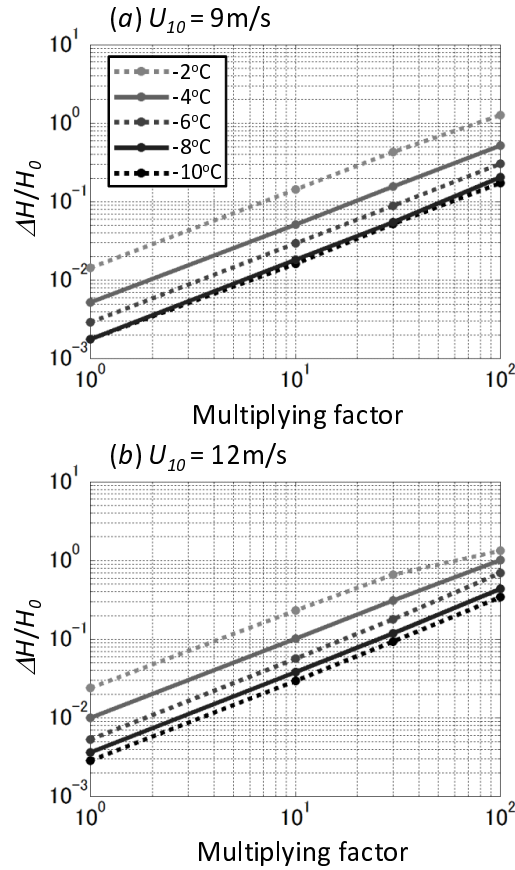


Figure 13: Relationship between the multiplying factor of SGF and fraction of heat flux difference with (a) $U_{10} = 9 \text{ ms}^{-1}$ and (b) $U_{10} = 12 \text{ ms}^{-1}$. Each plot represents a different air-sea temperature difference ($T_a - T_s$).

- Monahan, E., Spiel, D., Davidson, K., 1986. A model of marine aerosol generation via whitecaps and wave disruption. In: Monahan, E. C., Niocaill, G. M. (Eds.), *Oceanic Whitecaps*. Vol. 2 of *Oceanographic Sciences Library*. Springer Netherlands, pp. 167–174.
- Murray, F. W., 1967. On the computation of saturation vapor pressure. *J. Appl. Meteorol.* 6, 203–204.
- O'Dowd, C. D., de Leeuw, G., 2007. Marine aerosol production: A review of the current knowledge. *Phil. Trans. R. Soc. A* 365, 1753–1774.
- Perrie, W., Andreas, E. L., Zhang, W., Li, W., Gyakum, J., McTaggart-Cowan, R., 2005. Sea spray impacts on intensifying midlatitude cyclones. *J. Atmos. Sci.* 62, 1867–1883.
- Piazzola, J., Forget, P., Despiau, S., 2002. A sea spray generation function for fetch-limited conditions. *Annales Geophysicae* 20, 121–131.
- Piazzola, J., Forget, P., Lafon, C., Despiau, S., 2009. Spatial variation of sea-spray fluxes over a mediterranean coastal zone using a sea-state model. *Boundary-Layer Meteorology* 132 (1), 167–183.
- Saruwatari, A., Watanabe, Y., Ingram, D. M., 2009. Scarifying and fingering surfaces of plunging jets. *Coastal Engineering* 56, 1109–1122.
- Shpund, J., Pinsky, M., Khain, A., 2011. Microphysical structure of the marine boundary layer under strong wind and spray formation as seen from simulations using a 2D explicit microphysical model. Part I: The impact of large eddies. *Journal of the Atmospheric Sciences* 68 (10), 2366–2384.

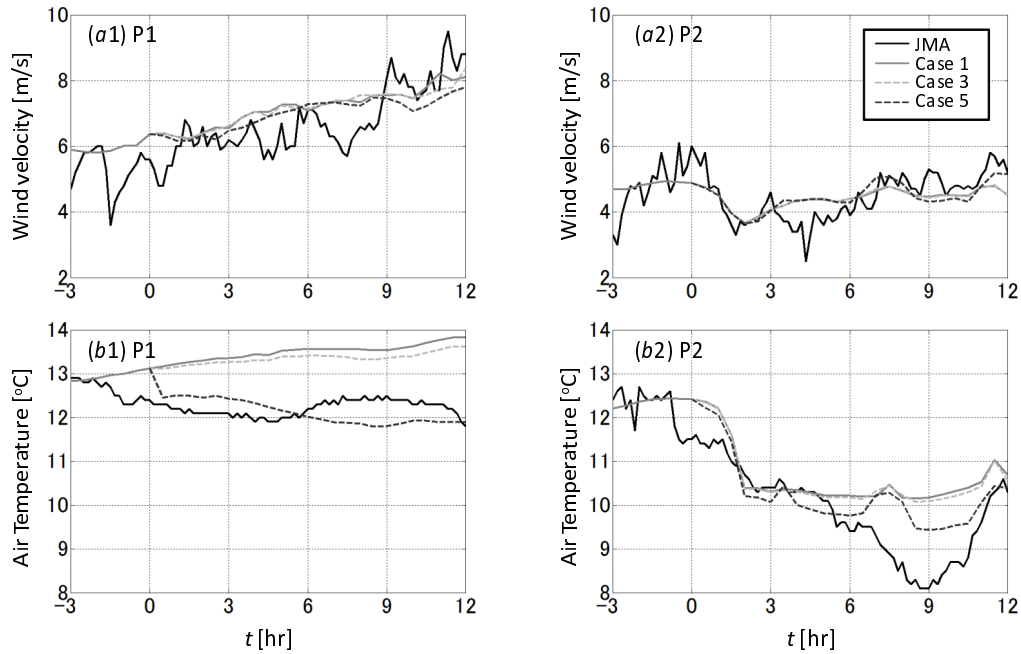


Figure 14: Comparison of the present results with observational data for (a) wind speed and (b) air temperature at the locations (1) P1, (2) P2 and (3) P3.

- Shpund, J., Zhang, J. A., Pinsky, M., Khain, A., 2012. Microphysical structure of the marine boundary layer under strong wind and spray formation as seen from simulations using a 2D explicit microphysical model. Part II: The role of sea spray. *Journal of the Atmospheric Sciences* 69 (12), 3501–3514.
- Spiel, D. E., 1998. On the birth of film drops from bubbles bursting on seawater surfaces. *J. Geophys. Res.* 103 (C11), 24907–24918.
- Ueda, M., 1960. Rate of evaporation of water by forced convection. *J. Appl. Phys. Japan* 29, 443–451.
- Ueda, M., 2000. *Humidity and Evaporation*. Corona Publishing Co. Ltd.
- van Eijk, A. M. J., Kusmierczyk-Michulec, J. T., Francius, M. J., Tedeschi, G., Piazzola, J., Merritt, D. L., Fontana, J. D., 2011. Sea-spray aerosol particles generated in the surf zone. *Journal of Geophysical Research: Atmospheres* 116 (D19).
- Veron, F., Hopkins, C., Harrison, E. L., Mueller, J. A., 2012. Sea spray spume droplet production in high wind speeds. *Geophysical Research Letters* 39 (L16602).
- Vickers, D., Mahrt, L., 2006. Evaluation of the air-sea bulk formula and sea-surface temperature variability from observations. *J. Geophys. Res.* 111 (C0502).
- Zhang, D.-L., Anthes, R. A., 1982. A high-resolution model of the planetary boundary layer-sensitivity tests and comparisons with SESAME-79 data. *J. Appl. Meteor.* 21, 1596–1609.